*Journal of The Electrochemical Society*, **158** (12) D710-D714 (2011)
0013-4651/2011/158(12)/D710/5/$28.00 © The Electrochemical Society

# Layer by Layer Etching of the Highly Oriented Pyrolythic Graphite by Using Atomic Layer Etching

**Y. Y. Kim,[a] W. S. Lim,[b] J. B. Park,[b] and G. Y. Yeom[a,b,z]**

[a]*Department of Advanced Materials Engineering and* [b]*SKKU Advanced Institute of Nano Technology (SAINT), Sungkyunkwan University, Suwon, Kyunggi-do 440-746, South Korea*

The layers of exfoliation graphene obtained by scotch taping of highly oriented pyrolythic graphite could be controlled precisely using an atomic layer etching (ALET) technology. Using the ALET, that is, by adsorbing oxygen radicals chemically on the graphene surface during the adsorption step and by removing the chemisorbed species only by Ar particle beam irradiation during the desorption step, exactly one monolayer of graphene could be removed during each etch cycle. The removal of each graphene layer by each ALET etch cycle could be observed through the optical microscope. In addition, the decrease of graphene layers could be also observed through the peak position change/broadening of G′ Raman peak. However, after the ALET, physical damage on the graphene surface could be also observed by the increase of D peak and decrease of G′ peak using the Raman spectra. The damaged graphene could be partially recovered by annealing at 1000°C for 30 minutes in 130 mTorr $H_2$/He environment.
 [DOI: 10.1149/2.061112jes] 

Manuscript submitted May 24, 2011; revised manuscript received September 13, 2011. Published November 14, 2011.

Recent ITRS (International Technology Roadmap for Semiconductors) roadmap shows that materials such as graphene, Ge, III–V semiconductor, and carbon nanotubes are emerging research device materials for the next generation devices which can replace silicon materials to decrease power consumption and to improve the performance of the device.[1] Among these materials, graphene which is composed of one or a few layers of carbon atoms with two dimensional hexagonal arrangement is investigated the most as the high speed semiconductor device materials because it has a high mobility of $3000 \sim 27000$ $cm^2$/Vs at room temperature and a high conductivity.[2]

Most of the graphene is fabricated by exfoliation of graphite crystal[3] or by chemical vapor deposition (CVD).[4] Among these, the exfoliation graphene which is obtained from highly oriented pyrolythic graphite (HOPG) flake is high quality graphene and shows higher mobility compared to the graphene grown by CVD, therefore, it is studied by many researchers as the ideal material for the investigation of the next generation graphene devices such as field effect transistor,[5] gas-sensor,[6] bio-sensor,[7] etc. Especially, the decrease of graphene layers from multilayer to monolayer decreases the interlayer scattering, and which increases the mobility sharply by the current modulation[8] and changes band structure.[9] Therefore, the control of the number of graphene layers is one of the important factors in controlling the electrical properties of graphene and the technique in controlling the graphene layer needs to be investigated.

The number of layers has been controlled by growing and stacking the monolayer CVD graphenes on a separate substrate,[4] or by etching the graphene by $O_2$ plasma,[10] or by removing the graphene layers through the oxidation at a high temperature,[11] etc. However, these methods are difficult to control the layers of graphene precisely and locally which is beneficial in fabricating graphene devices. Recently, a technique to remove a monolayer graphene only on a local area by selectively depositing Zn on graphene layers followed by treating in a HCl solution has been reported for device patterning.[12] Atomic layer etching (ALET) is believed to be another technique that can remove the graphene layer-by-layer and selectively on local areas. It removes one atomic layer of graphene per etch cycle by adsorption of chemical reactants followed by desorption of the chemisorbed species.[13] In this study, the HOPG graphene layer was etched by ALET technology and its effect on the controlling the layer of the HOPG graphene was investigated especially as a method to control the layers of graphene precisely and selectively.

## Experimental

The etch cycle of graphene ALET composed of four steps is shown in Figure 1. As shown in Fig. 1, $O_2$ radicals are adsorbed on the graphene surface during the 1st adsorption step, and where the graphene surface is chemisorbed by oxygen. The remaining $O_2$ radicals are purged by 2nd evacuation step. The chemisorbed carbon on the graphene surface (CO) is desorbed by Ar particle bombardment during the 3rd desorption step, and the remaining Ar and chemiscorbed species are purged by the 4th evacuation step.

For the adsorption of $O_2$ radicals and for the desorption of chemisorbed carbon on the graphene surface, a neutral beam assisted ALET equipment consisted of a three-grid inductively coupled plasma (ICP) ion gun and a parallel low angle reflector installed in front of the ICP ion gun for the neutralization of the extracted ions from the ion gun was used. The reflector plate was tilted 5° from the ion beam direction to neutralize the ions extracted from the ICP ion gun by the low angle reflection of the ions on the reflector. The details of the ALET source are described in detail elsewhere.[14] During the desorption step, +30 V, −150 V, and 0 V were applied to the first grid(acceleration grid; the voltage controls the energy of the extracting ions and it is located close to the ICP source), second grid (focusing grid; controls flux of the ions), and third grid (deceleration grid; located close to the reflector plate), respectively, while applying 300 W rf power to the ICP source and supplying 30 sccm Ar gas to the source. In the case of the adsorption of $O_2$ radical, all the grid voltages were set at 0V for the radical extraction while applying 300 W of 13.56 MHz rf power to the ICP source and supplying 20 sccm $O_2$ gas to the source.

A few layer thick exfoliation graphene was obtained by scotch taping the HOPG and transferring on the $SiO_2$(300 nm)/silicon substrate. The layers of graphene before and after the etching by ALET were observed by optical microscope and the characteristics of the graphene were observed by Raman spectroscopy (514 nm Raman, Renishaw-Invia Basic) The carbon binding energy of the graphene surface etched by ALET was observed by X-ray photoelectron spectroscopy(XPS, Thermo VG, MultiLab 2000, Mg Kα source) at the take-off angle of 60° using HOPG itself with the size of 1 cm×1$cm^2$. The carbon bonding energy peak of HOPG surface was deconvoluted using Avantage 3.95-surface chemical analysis program by Thermo Fisher Scientific Inc.

## Results and Discussion

The chemical binding states of carbon on the HOPG surface were investigated by XPS after the adsorption of $O_2$ radical and after the desorption of the chemisorbed carbon by Ar particle beam irradiation

[z] E-mail: gyyeom@skku.edu

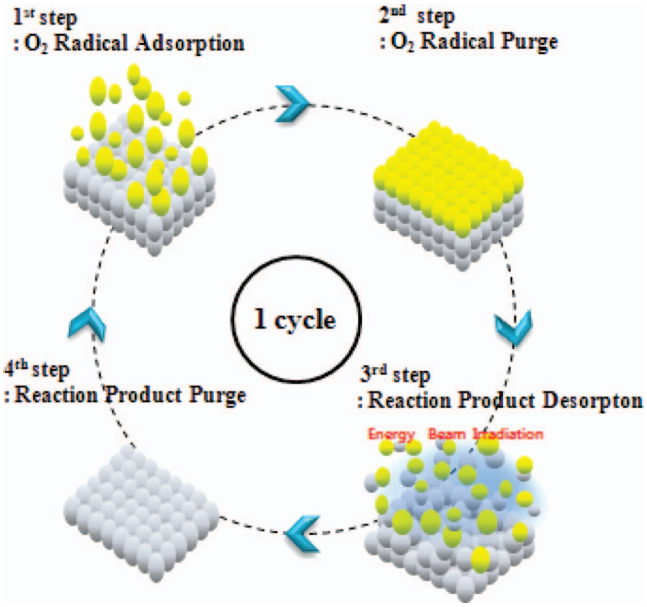


**Figure 1.** Concept of four step graphene ALET cycle.

and the results are shown in Figure 2 Figure 2a shows XPS C1s data of HOPG surface after each step of the etch cycles (reference, after oxygen chemisorption, after 1cycle ALET, and after annealing) and Figure 2b shows the atomic percentage (%) of carbon bondings ($sp^2$, $sp^3$, and C–O) on the HOPG surfaces obtained after the deconvolution of the XPS C1s data in Figure 2a.[15,16] During the adsorption of $O_2$ radical, the HOPG was exposed to the $O_2$ radical for 5minutes. As shown in Figure 2b, before the etching, the carbon bonding on the HOPG surface was composed of $sp^2$ C–C bonding at 284.6 eV (87 atomic %) and $sp^3$ C–C bonding at 285.7 eV (13 atomic %). After the adsorption of $O_2$ radical (that is, oxygen atom), $sp^2$ C-C bonding decreased to 60% while increasing $sp^3$ C-C bonding to 28%. In addition, 12 atomic % of C-O bonding at 288 eV could be observed. Therefore, after the adsorption of $O_2$ radical, about 27 atomic% of $sp^2$ C-C bonding changed to C-O binding and $sp^3$ C-C bonding. The change of $sp^2$ C-C bonding to C-O bonding and $sp^3$ bonding appears to be partially related to the chemisorption of oxygen to carbon.

To etch monolayer graphene, uniform monolayer C-O bonding should be formed on the HOPG surface. However, due to the depth resolution of XPS, even though XPS data was obtained at the take-off angle of 60°, it was difficult to figure out whether the monolayer C-O bonding was formed or not by XPS. When monolayer C-O bonding was not formed on the HOPG surface, the percentage of C-O bonding on the HOPG surface is increased with the increase of the exposure time to $O_2$ radicals and, if the uniform monolayer C-O bonding is formed on the HOPG surface, then, the percentage of C-O bonding on the HOPG surface will be saturated. Therefore, to figure out whether the C-O bonding is saturated on the HOPG surface or not by the formation of monolayer C-O bonding, the atomic percentage of C-O bonding on the HOPG surface was measured by XPS with increasing $O_2$ radical exposure time and the result is shown in Figure 3 In Fig. 3, in addition to the atomic percentages of C-O bonding, the atomic percentages of $sp^3$ C-C bonding and $sp^2$ C-C bonding are also shown as a function of $O_2$ radical exposure time. As shown in the figure, the C-O bonding percentage was increased with the increase of $O_2$ radical exposure time in addition to the increase of $sp^3$ C-C bonding percentage and the decrease of $sp^2$ C-C bonding percentage. The

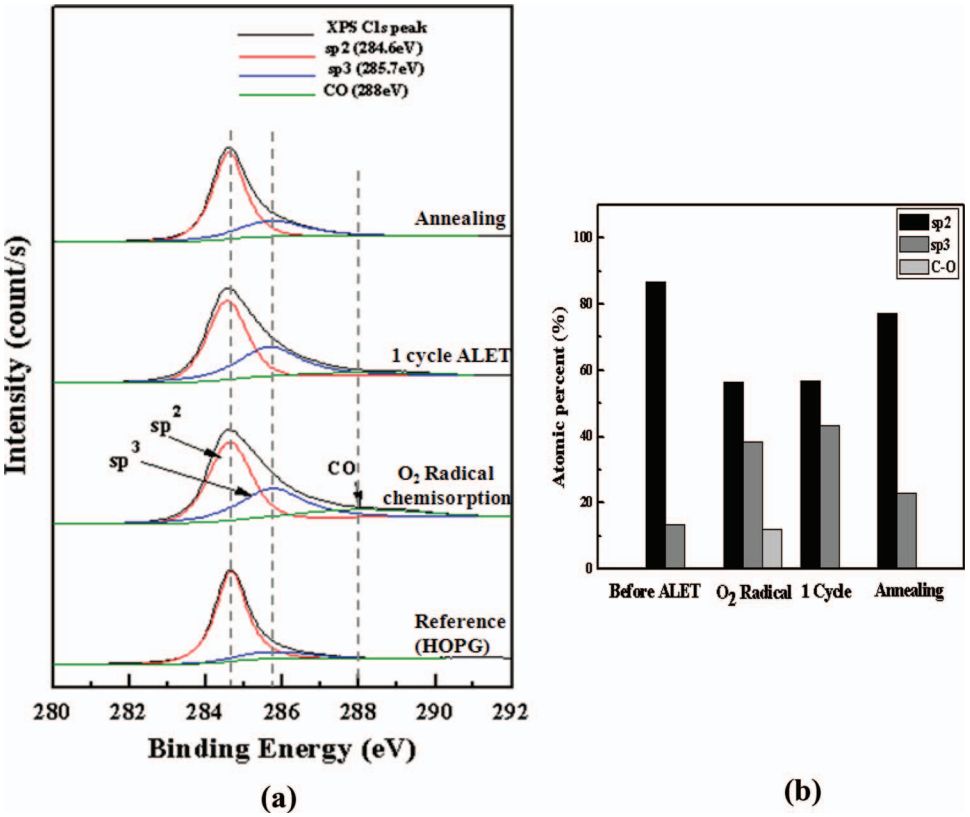


**Figure 2.** (a) XPS C1s data of HOPG surface after each step of the etch cycles (reference, after oxygen chemisorption, after 1cycle ALET, and after annealing). (b) Atomic percentage (%) of carbon bondings ($sp^2$, $sp^3$, and C-O) on the HOPG surfaces obtained after the deconvolution of the XPS C1s data in Figure 2a. Observed graphene surface was measured by XPS at the take off angle of 60°.

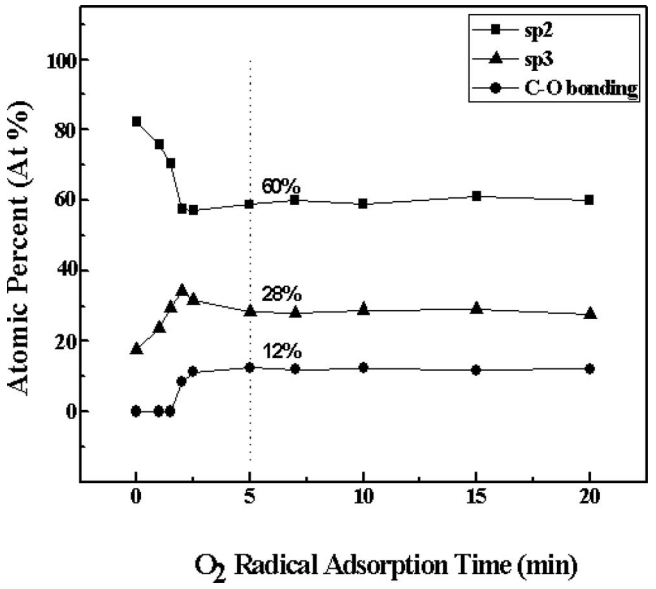


**Figure 3.** Atomic percentage (%) of carbon bondings ($sp^2$, $sp^3$, and C-O) on the HOPG surface measured after the chemical adsorption step as a function of $O_2$ radical exposure time by XPS at the take off angle of 60°.

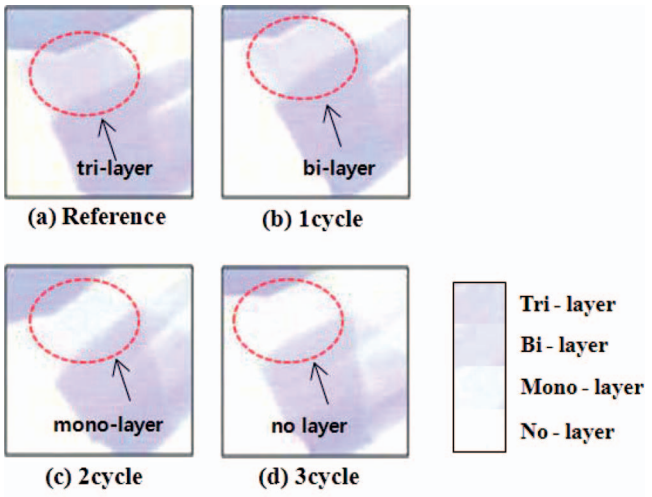


**Figure 4.** Optical images of exfoliation graphene on $SiO_2$/Si measured as a function of ALET cycles. (a) trilayer graphene before ALET of graphene (Si/$SiO_2$(300 nm)/graphene) (b) After 1 cycle ALET, bilayer graphene surface after the removal of one layer graphene (c) After 2 cycle ALET, monolayer graphene surface after the removal of two graphene layers. (d) After 3 cycle ALET, no graphene on Si/$SiO_2$ after the removal of three layers of graphene.

C-O bonding percentage was saturated at about 5 minutes and no further increase of C-O bonding percentage indicating the formation of a monolayer C-O bonding on the HOPG surface. The saturation of $sp^3$ C-C bonding percentage and $sp^2$ C-C bonding percentage also supports the formation of a monolayer C-O bonding on the HOPG surface.

The monolayer C-O bonding on the HOPG surface needs to be completely removed by the following Ar beam irradiation step. As shown in Fig. 2, after the Ar beam irradiation for 1 minute, the carbon binding state of HOPG surface changed to 57 atom % of $sp^2$ C-C bonding and 43 atom % of $sp^3$ C-C bonding and no C-O bonding could be observed. Therefore, after the Ar beam irradiation, the chemisorbed carbon (C-O bonding) was desorbed completely. However, after 1 cycle of ALET, the $sp^3$ bonding formed after the $O_2$ radical adsorption, was not recovered to $sp^2$ C-C bonding, and it is believed to be partially related to the damage of the graphene substrate during the $O_2$ radical adsorption and Ar beam irradiation. The recovery of the graphene surface could be observed after the annealing of the etched graphene ($H_2$ : He gas mixture flow ratio 42:1, 130 mTorr, 1000°C, 30 min). As shown in Fig. 2, after the annealing of the etched graphene surface, $sp^2$ bonding percentage increased about 20% (from 57% to 77%) while decreasing $sp^3$ bonding percentage to 23% by the rearrangement of the carbon atoms to $sp^2$ bonding.[15] Even though the $sp^2$ bonding percentage after the annealing was lower than that of as-is, the significant recovery of the damaged graphene surface could be obtained after the annealing.

After each ALET cycle, the graphene was observed by an optical microscope and Raman spectroscopy to examine the removal of graphene layers. Figure 4 shows the graphene surface observed (a) before etching (reference), (b) after 1cycle ALET, (c) after 2 cycle ALET, and (d) after 3 cycle ALET. The circled area of the reference sample in Fig. 4a was determined to be trilayer graphene by Raman spectroscopy. After the 3 cycle ALET, the graphene in the circled area was completely removed as shown in Fig. 4d. Also, as shown in Figs. 4b and 4c, with the increase of ALET cycle, the optical transmittance of the graphene layers was increased indicating the decrease of the graphene layer to bilayer for Fig. 4b and monolayer for Fig. 4c with the increase of ALET cycle. Therefore, one graphene layer etching per one ALET cycle could be obtained. (As a further evidence of one graphene layer etching per one ALET cycle, a bi-layer graphene prepared by a mutliple transfer technique of chemical vapor deposited monolayer graphene was etched using ALET and the optical transmittance was measured. The result showed the decrease of 2.3% optical transmittance at 550 nm after one ALET cycle which corresponds to the optical absorption percentage of one monolayer graphene. The results are not shown.)

The removal of the HOPG layer during the ALET could be confirmed by observing the graphene layer surface by Raman spectroscopy. Figure 5a shows the Raman spectra of the exfoliation graphene layers after each ALET cycle for 4 cycles in addition to the Raman spectrum of the reference. Before the etching, the graphene layers were determined to be 4 layers. Also, after the each ALET cycle, the graphene surface was annealed at the condition in Fig. 2 before the further etching by ALET. Raman spectroscopy was measured at the same position. As shown in the figure, the etched graphene showed D band near 1350 $cm^{-1}$, G band near 1580 $cm^{-1}$, shoulder D′ band[17] near 1615 $cm^{-1}$, and G′ band at 2660 ~ 2726 $cm^{-1}$. As shown in the Raman spectrum of the reference, the perfect exfoliation graphene did not show the D band peak at near 1350 $cm^{-1}$ and the D band peak is related to the formation of defect and cutting-off $sp^2$ bonding on the graphene lattice. Therefore, the formation of D band peak in Fig. 5a is believed to be related to the disorder of the graphene lattice during the $O_2$ radical adsorption and Ar beam irradiation.[18] The shoulder D′ band peak is also related to the defect on the graphene caused by the intervalley double-resonant Raman scattering.[19,20] After the annealing, the D peak intensity and shoulder D′ intensity were decreased significantly while increasing the G band peak intensity and the G′ band peak intensity indicating recovery of the damaged graphene by the annealing. The change of G band peak intensity and the G′ band peak position/intensity is also related to the thickness of graphene layers. As shown in the figure, with the increase of etch cycles, the G band peak intensity and G′ band peak intensity were decreased and the G′ peak position was also changed even after the annealing indicating the decrease of graphene layer with the increase of etch cycle.

The D band peaks of the exfoliation graphene layers after the ALET cycles and after the annealing in Fig. 5a are shown in more detail in Figure 5b. As shown, as the etch cycle increases from 1 to 3, the D band peak intensity decreased slightly to lower frequency by showing 1354 $cm^{-1}$ after 1 ALET cycle, 1345 $cm^{-1}$ after 2 ALET cycles, and 1340 $cm^{-1}$ after 3 ALET cycles. The D band peak appears to be related to the different graphene layers (that is, the D band peak observed at 1354 $cm^{-1}$ after 1 ALET cycle is related to trilayer graphene, that

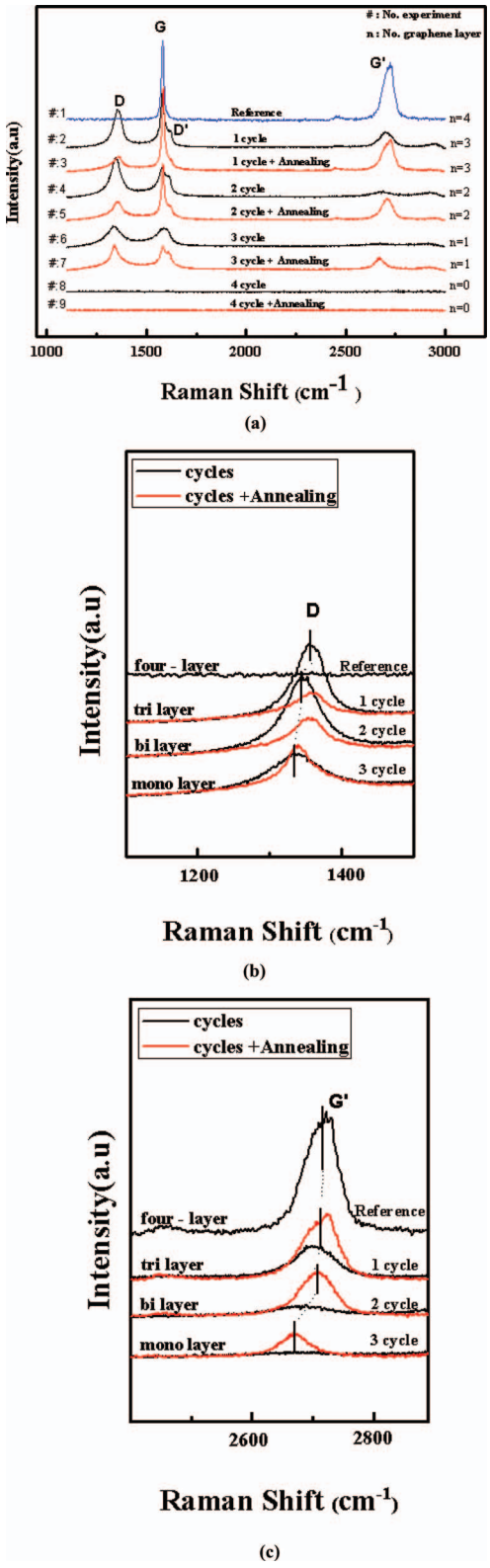


**Figure 5.** (a) Raman spectra showing the intensity of D, G, and G′ band peaks. The Raman spectra were measured as a function of ALET cycle and after the annealing (#: experimental numbers, n = graphene layer numbers). Annealing condition : $H_2$:He (42:1) gas mixture, 300 mTorr at 1000°C for 30 min). (b) Comparison of D band peak intensities of the exfoliation grahene layers after the ALET cycles and after the annealing of the etched graphene layers. (c) Comparison of 2D (G′) band peak intensities of the exfoliation graphene layers after the ALET cycles and after the annealing of the etched grahene layers.

at 1345 $cm^{-1}$ after 2 ALET cycles is to bilayer graphene, and that at 1340 $cm^{-1}$ after 3 ALET cycles is to monolayer graphene) even though the reason for the decrease in the frequency of the D band peak for the smaller number of graphene layers is not clear. After the annealing, the D band peak was not changed significantly, however, the peak intensity was decreased significantly due to the recovery of the graphene defects as observed by XPS in Fig. 2. However, even after the annealing, the small D band peak intensity still remains indicating incomplete recovery of graphene defect possibly due to the lack of carbon for the full recovery on the graphene surface during the annealing.

The G′ band peaks of the graphene layers after the ALET cycles and after the annealing in Fig. 5a are shown in Figure 5c in more detail. The shapes and frequency of the G′ band are known to be sensitive to the number of graphene layers.[18] As shown in Fig. 5c, after the ALET, the observed intensity of the G′ band peak was very small and, in the case of the graphene after 3 clycles of ALET, the peak was not even noticeable. The G′ peak positions after 1 cycle ALET and 2 cycle ALET were 2700 $cm^{-1}$ and 2687 $cm^{-1,}$ respectively. Therefore, similar to the D peak position, the G′ band peak position was also changed to lower frequency with the increase of etch cycles. After the annealing, the G′ peak intensity was increased indicating the recovery of the graphene crystallinity. In addition, the peak positions were changed to higher frequency of 2715 $cm^{-1}$, 2707 $cm^{-1}$, and 2671 $cm^{-1}$ after the annealing of graphene etched by ALET for 1 cycle, 2 cycles, and 3 cycles, respectively.[21] The peak positions are similar to the G′ peak positions for trilayer graphene, bilayer grapehene, and monolayer graphene, respectively.[22] Therefore, the etching of one graphene monolayer by 1 cycle ALET could be confirmed. Also, the G′ peak positions measured before the annealing after the 1 cycle ALET (2700 $nm^{-1}$), 2 cycle ALET(2687 $nm^{-1}$), and 3 cycle ALET (no peak) were similar to the G′ peak positions of bilayer graphene, monolayer graphene, and no grpahene, respectively. Therefore, it is believed that, after the each ALET, top one grahene layer has transformed to a nanocrystalline state[23] by C-C bond breaking and the removal of some carbon atoms through the Ar beam irradiation. However, after the annealing, the G′ peak position has moved to that of graphene with one more layer by recovering the broken C-C bonding through the annealing. Therefore, through the Raman spectroscopy, the control of the exact graphene layer thickness by the ALET could be observed even though the perfect recovery of the graphene surface defects formed during the ALET could not be achieved after the annealing as shown in Figs. 5b and 5c.

## Conclusions

In this study, a graphene etching technology which can precisely control one graphene layer has been investigated by etching the HOPG using an ALET technology, where, the graphene surface layer is chemisorbed by $O_2$ radical adsorption and the chemisorbed C-O bonding layer on the HOPG is removed by following Ar beam irradiation. The chemisorptions of the $O_2$ radical on the HOPG surface could be observed by XPS by decreasing the $sp^2$ C-C bonding percentage about 27% and by increasing the $sp^3$ C-C bonding percentage about 15% in addition to the formation of C-O bonding percentage about 12%. After the Ar beam irradiation, the formed C-O bonding was completely removed while keeping $sp^2$ C-C bonding percentage indicating the complete removal of chemisorbed species on the graphene surface, that is, the removal of one graphene layer by one etch cycle. The removal of one graphene layer by one ALET cycle could be also confirmed by optical microscope and Raman spectroscopy. However, after the ALET, the physical damage on the etched graphene surface could be observed by the increase of $sp^3$ bonding percentage for XPS and by the increase of D band peak intensity for Raman spectroscopy. The damaged layer appears to be limited to one surface graphene layer and most of the defects could be recovered by the annealing for 30 min at 1000°C in a 130 mTorr $H_2$/He gas mixture. It is believed that the ALET technology can be useful in making a all-carbon device, where, source and drain are composed of multilayer conductive

graphene, and gate graphene layer is selectively reduced to bilayer by the ALET to form semiconducting graphene.

## Acknowledgment

This work was supported by the National Research Foundation of the Korea Grant funded by Korean Government (MEST) (2010-0026248).

## References

1. The International Technology Roadmap for Semiconductors: 2009 Emerging Research Materials.
2. K. S. Novoselov, A. K. Geim, S. V. Morozov, D. Jiang, Y. Zhang, S. V. Dubonos, I. V. Grigorieva, and A. A. Firsov, *Science*, **306**, 666 (2004).
3. A. K. Geim, and K. S. Novoselov, *Nat. Mater.*, **6**, 183 (2007).
4. K. S. Kim, Y. Zhao, H. Jang, S. Y. Lee, J. M. Kim, K. S. Kim, J.-H. Ahn, P. Kim, J.-Y. Choi, and B. H. Hong, *Nature*, **457**, 706 (2009).
5. F. Schwierz "Graphene transistors" *Nat. Nanotechnol*., **5** (2010).
6. G. Ko, H.-Y. Kim, J. Ahn, Y.-M. Park, K.-Y. Lee, and J. Kim, *Cur. Appl. Phys.*, **10**, 1002 (2010).
7. F. Rose, P. Martin, H. Fujita, and H. Kawakatsu, *Nanotechnol.*, **7**, 3325 (2006).
8. K. Nagashio, T. Nishimua, Koji, and A. Toriumi, *Appl. Phys. Exp.*, **2**, 02533 (2009).
9. H. Raza and E. C. Kan, *J. Phys.: Condens. Matt.*, **21**, 102202 (2009).
10. X. Lu, H. Huang, N. Nemchuk, and R. S. Ruoff, *Appl. Phys. Lett.*, **75**, 193 (1999).
11. L. Liu, S. Ryu, M. R. Tomasik, E. Stolyarova, N. Y. Jung, M. S. Hybertsen, M. L. Steigerwald, L. E. Brus, and G. W. Flynn, *Nano Lett.*, **8**, 1965 (2008).
12. A. Dimiev, V. Kosynkin, A. Sinitskii, A. Slesarev, Z. Sun, and J. M. Tour, *Science*, **331**, 1168 (2011).
13. S. D. Park, C. K. Oh, J. W. Bae, G. Y. Yeom, T. W. Kim, J. I. Song, and J. H. Jang, *Appl. Phys. Lett.*, **89**, 043109 (2006).
14. D. H. Lee, J. W. Bae, S. D. Park, and G. Y. Yeom, *Thin Solid Films.*, **398**, 647 (2001).
15. C. Mattevi, G. Eda, S. Agnoli, S. Miller, K. A. M. khoyan, O. Celik, D. Mastrogiovanni, G. Granozzi, E. Garfunkel, and M. Chhowalla, *Adv. Fun. Mater.*, **9**, 2577 (2009).
16. R. Haerle, E. Riedo, A. Pasquarello, and A. Baldereschi, *Phys.Rev. B*, vol. **65**, 045101 (2001).
17. D. C. Elias, R. R. Nair, T. M. G. Mohiuddin, S. V. Morozov, P. Blake, M. P. Halsall, A. C. Ferrari, D. W. Boukhvalov, M. I. Katsnelson, A. K. Geim, and K. S. Novoselov, *Science*, **323**, 5914 (2009).
18. A. Gupta, G. Chen, P. Joshi, S. Tadigadapa, and P. C. Eklund, *Nano Lett.*, **6**, 2667 (2006).
19. L. G. Cancado, M. A. Pimenta, B. R. A. Neves, M. S. S. Dantas, and A. Jorio1, *Phys. Rev. Lett.*, **93**, 247401 (2004).
20. A. C. Ferrari, J. C. Meyer, V. Scardaci, C. Casiraghi, M. Lazzeri, F. Mauri, S. Piscanec, D. Jiang, K. S. Novoselov, S. Roth, and A. K. Geim, *Phys.Rev. Lett.*, **97**, 187401 (2006).
21. D. Graf, F. Molitor, K. Ensslin, C. Stampfer, A. Jungen, C. Hierold, and L. Wirtz, *Nano lett.*, **7**, 238 (2007).
22. L. M. Malard, M. A. Pimenta, G. Dresselhaus, and M. S. Dresselhaus, *Phys. Repor.*, **473**, 51 (2009).
23. A. C. Ferrari and J. Robertson, *Phil. Trans. R. Soc. Lond. A*, **362**, 2477 (2004).